NUCLEAR ENGINEERING HANDBOOK

A collection of notes from the master of science in nuclear engineering

Pagliuca Simone
simone@pagliuca.net

Track: Nuclear Power Plants
Academic years: 2023∼2025

INTRODUCTION: lorem ipsum dolor sit amet, consectetur adipiscing elit. Donec auctor, nunc nec ultricies ultricies, nunc nunc.

Contents

I Experimental Reactor Kinetics

1 Control Rods

1.1 Introduction to Control Rods

1.1.1 Functions

Control rods are essential for **modulating reactivity**, serving the following functions:

- Compensating for excess reactivity due to fuel consumption or thermal feedback
- Regulating the neutron population
- Providing a safety margin for shutdown
- Assisting in reactor startup

1.1.2 Physical Behavior

Control rods function as **neutron absorbers** by altering the absorption component of K_{eff}:

$$K_{eff} = \frac{Production}{Absorption + Leakages} = \frac{\int\int \nu\Sigma_f \phi dV dE}{\int\int_{fuel} \Sigma_a \phi dV dE + \dot{L}} \tag{1.1}$$

1.1.3 Effects

The insertion of a control rod modifies the neutron flux distribution as shown in figure 1.1. Its effectiveness depends on its absorption capability and the neutron flux in its vicinity.

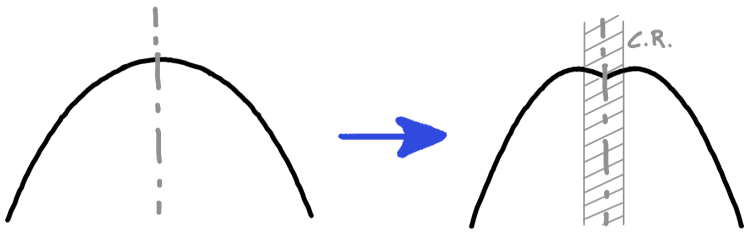

Figure 1.1: Flux before and after control rod insertion

Shadowing effect: The position of one control rod can impact the effectiveness of another.

1.1.4 Design

The **material** selection is critical, requiring a substance with high absorption capabilities. For example, B^{10} primarily undergoes (n,α) reactions, while Gadolinium is more likely to produce (n,γ) reactions, which raises radiological safety concerns.
Following material selection, the **rod geometry** is typically constrained by overall design parameters.
Finally, the required **number of rods**, or equivalently the pcm, is determined by the need to compensate for excess reactivity at the start of the fuel cycle and provide an adequate shutdown margin. This depends on the core design and technology. For istance the difference between the excess reactivity over time in a conventional burner reactor agaist a breeeder reactor (shown in fig. 1.2) shows the difference is needed reactivity compensation.

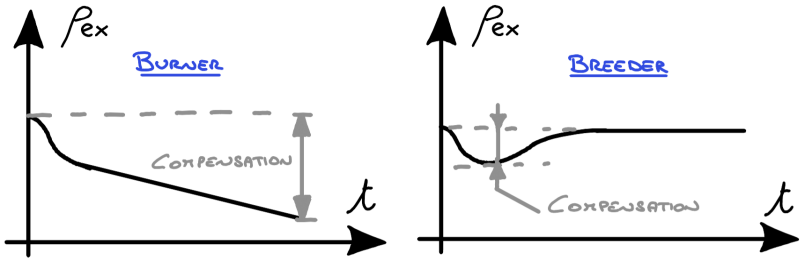

Figure 1.2: Reactivity worth needed for fuel consumption compensation is generally lower in breeder reactors compared to burner reactors.

1.1.5 Calibration

Calibration is necessary because the reactivity introduced by a control rod is not directly proportional to its insertion depth; instead, effectiveness varies with insertion depth, as illustrated in the following graphs:

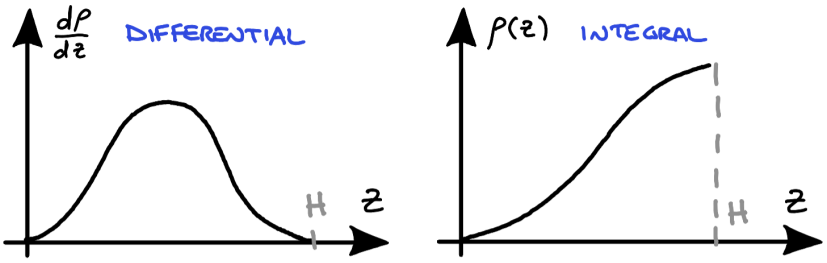

Figure 1.3: Differential and Integral reactivity curves

1.1.6 Formulas

The total reactivity worth ($\Delta\rho_{TOT}$) is given by:

$$\Delta\rho_{TOT} = \Delta\rho_{SM} + \Delta\rho_{EX} \tag{1.2}$$

where $\Delta\rho_{SM}$ is the shutdown margin and $\Delta\rho_{EX}$ is the reactivity excess.

Shutdown Margin:

$$\Delta\rho_{SM} = \rho_i(\text{Criticality}) - \rho_i(\text{Fully IN}) \tag{1.3}$$

Reactivity excess:

$$\Delta\rho_{EX} = \rho_i(\text{Fully OUT}) - \rho_i(\text{Criticality}) \tag{1.4}$$

1.2 Critical Calibration Method

1.2.1 Theory

The calibration of control rods in a reactor is crucial for understanding their reactivity worth. This can be accomplished using the in-hour and point kinetics equations to relate the time required to increase power by a factor to the reactivity.

Reactivity and Reactor Period

The relationship between reactivity (ρ) and the reactor period (T) is fundamental in control rod calibration. The point kinetics equations describe this relationship:

$$\frac{dP}{dt} = \frac{\rho - \beta}{\Lambda} P + \sum_{i=1}^{6} \lambda_i C_i \tag{1.5}$$

$$\frac{dC_i}{dt} = \frac{\beta_i}{\Lambda} P - \lambda_i C_i \tag{1.6}$$

where:

- P is the reactor power,
- ρ is the reactivity,
- β is the delayed neutron fraction,
- Λ is the prompt neutron lifetime,
- β_i and λ_i are the delayed neutron fractions and decay constants for each of the six precursor groups,
- C_i is the concentration of the i-th delayed neutron precursor group.

We can measure the reactor period T by inserting a control rod and observing the time required for the reactor power to increase by a factor e.
In practice we will use a factor 1.5 and compute the period as $T = \frac{\Delta t}{ln(1.5)}$.
We can then take advantage of the in-hour equation to correlate the reactivity to the reactor period:

$$\rho = \frac{\Lambda}{\mathbf{T}} + \sum_{i=1}^{6} \frac{\beta_i \lambda_i}{1 + \lambda_i \mathbf{T}} \tag{1.7}$$

We are going to use a 6 group apprach, the values of β_i and λ_i are known from montecarlo simulations and therefore come with their own uncertanty.

1.2.2 Pros and Cons of the Critical Method

Advantages:

- Absolute method: results are independent of other factors, including the position of other control rods
- High accuracy of results

Disadvantages:

- Time-intensive, as calibration is required for each control rod
- Reactor remains in supercritical condition during measurements

1.2.3 Experimental Procedure

Starting with a reactor in cold and clean conditions to avoid effects due to external poisons or thermal feedback.

1. Bring the reactor to a critical state.
2. Raise the REG rod by some steps
3. Measure the time required for the power to increase $3W \rightarrow 4.5W$.
4. Measure the time required for the power to increase $6W \rightarrow 9W$.
5. Adjust the shim rod to get back to criticality.
6. Repeat until the REG rod is fully withdrawn.

It is worth noting that the first measurment $3W \rightarrow 4.5W$ will take into also precursors, by the time of the second measurment most of them will be decayed so the measurment should be more rapresentative of the reactiviy.

1.3 Subcritical Control Rod Calibration

1.3.1 Introduction

The subcritical method provides an alternative approach to control rod calibration, particularly useful for cases where safety is a concern. This method allows for calibration while keeping the reactor in a subcritical state by using an external neutron source.

1.3.2 Theory - TBC

Subcritical Multiplication and Reactor Period

In subcritical conditions, the neutron population depends on both the external source and the reactor's multiplication factor K_{eff}. This dependency is described by the subcritical multiplication factor M:

$$M = \frac{1}{1 - K_{eff}} \tag{1.8}$$

With an external source, the neutron population evolves over generations until it reaches a steady state. This evolution can be described by a geometric series with K_{eff} as the ratio, where the number of generations required to reach steady state is:

$$N_{\text{steady}} \approx \frac{4}{\ln K} \tag{1.9}$$

Which means that the evolution is slower the closer we get to the steady state condition.

Point Kinetics Equations

To understand the reactor's response over time, we use the point kinetics equations adapted for the subcritical state:

$$\frac{dn}{dt} = K_{eff}\left(\frac{K_{eff} - 1}{K_{eff}} + \rho - \beta\right)\frac{n}{\Lambda} + \sum \lambda_i C_i + q \tag{1.10}$$

$$\frac{dC_i}{dt} = K_{eff}\frac{\beta_i}{\Lambda}n - \lambda_i C_i \tag{1.11}$$

where $\rho = \frac{\Lambda}{K}$ and q is the source term. The reactor period T is then given by:

$$T = \frac{1}{\lambda_1} \tag{1.12}$$

1.3.3 Experimental Procedure

The following steps outline the subcritical calibration procedure:

1. Bring the reactor in subcritical condition with all rods inserted.
2. Measure the neutron rate $\dot{R}$, we used a fission chamber, in pulse mode.

3. Insert the source and measure $\dot{R}$ again, we used $Ra\text{-}Be_r$.
4. Extract the control rods of which we know its reactivity worth and measure $\dot{R}$ once it reached steady state.
5. Compute the subcritical multiplication factor of the CR from known reactivity worth: $\Delta\rho = \rho_{out} - 0 = \frac{K-1}{K} \rightarrow M = \frac{1}{1-K}$.
6. Compute the calibration parameter $\alpha\Phi_s$ from this measurment: $\frac{\dot{R}}{M} = \alpha\Phi_s$.
7. Reinsert the control rod.
8. Extract another control rod and measure $\dot{R}$.
9. Compare measured $\dot{R}$ to the calibration parameter: $M = \alpha\Phi_s\dot{R}$
10. Repeat the last two steps for all control rods.

For better statistics take multiple measurements for each control rod (or long measurements).

> **Note on statistics**: In poisson distributed data like radiation counts taking 20 short measurments each of time t will give the same statistical error as taking 1 longer measurement of time $T = 20t$.

1.3.4 Pros and Cons of the Subcritical Method

Advantages:

- Safe and keeps the reactor subcritical.
- Allows calibration of the shim, unlike other methods.

Disadvantages:

- Relys on the knowledge of one control rod's reactivity worth.
- Lower accuracy due to reliance on source and instrumentation.
- Only measures the total worth of the control rod, unable to get the full integral curve with reasonable measuring time (if we do a small step the variation in count rate change can easly hide in the noise and error).
- Frequent recalibration required due to burnup of fission chamber.

2 Reactivity Coefficients

2.1 Definition

The reactivity coefficient, denoted as α, is defined as:

$$\alpha = \frac{\partial \rho}{\partial x} \tag{2.1}$$

where x represents a certain quantity that affects the reactivity, ρ.

2.2 Reactivity Coefficients for Different Components

For our case, we consider the following reactivity coefficients.

- α_f = Fuel reactivity coefficient
- α_m = Moderator reactivity coefficient
- α_c = Coolant reactivity coefficient
- α_e = Reactivity due to thermal expansion of the fuel

In the TRIGA reactor, α_e can often be neglected because, as in other thermal systems, the thermal expansion is smaller compared to the migration length of neutrons.

Note for fast reactors: The higher migration length in fast reactors makes the reactivity effect of thermal expansion more relevant.

2.3 Doppler Effect

The fuel reactivity coefficient, α_f, is primarily due to the Doppler effect. The Doppler effect causes a broadening of the resonance peaks in the absorption cross-section of the fuel.

$$\sigma(\text{fuel, E}) = \text{Doppler Effect} \tag{2.2}$$

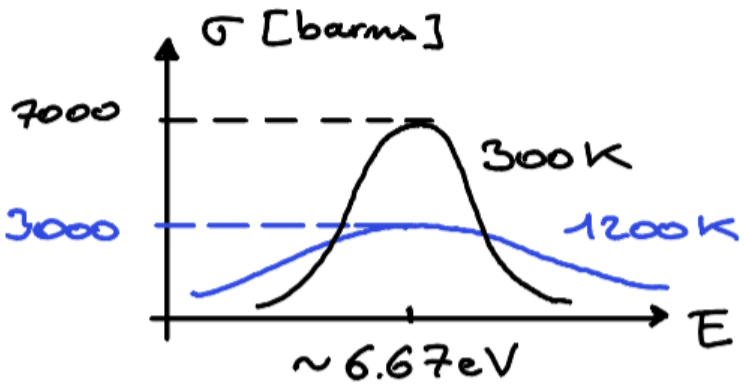

Figure 2.1: The Doppler effect shows the broadening of resonance peaks.

2.4 Functions of Reactivity Coefficients

Specifically for the TRIGA reactor:

- $\alpha < 0$ indicates a **negative reactivity coefficient**, which is essential for safety.
- $\alpha \ll 0$ allows for stable operation in *pulse mode*.

2.5 Design Considerations

When designing a system with fuel and moderator, consider the following:

- Increase in temperature ($T \uparrow$) leads to reduced moderation capability, affecting the neutron flux.
- The effect on the absorption cross-section ($\Sigma_a \downarrow$) also reduces the reactivity.

2.6 Physical Background

The physical background involves the following dynamics:

$$\frac{dn}{dt} = P - A - L + S \tag{2.3}$$

where:

- P denotes production, which depends on $\Sigma_f \phi$

- A denotes absorption, proportional to $\Sigma_a \phi$
- L denotes leakage, related to $\nabla D \phi$
- S denotes scattering, related to $\Sigma_s \phi$

The reactivity ρ can be approximated by:

$$\rho \propto \frac{P - A - L}{P} \tag{2.4}$$

2.6.1 Dependence on Parameters

The parameters affecting reactivity are:

- Temperature (affects cross-section and density)
- Geometry (affects distribution)
- Fuel condition (corrosion, burnup, etc.)

2.6.2 Side Note on Fast Reactors

In fast reactors, the coefficients α_f and α_c can be greater than zero depending on the fuel composition, as is the case with molten salt reactors where fuel is mixed with the coolant.

2.7 Overview of the Effects of Reactivity Coefficients

The following plot gives an overview of how reactivity feedbacks affect power in the reactor.

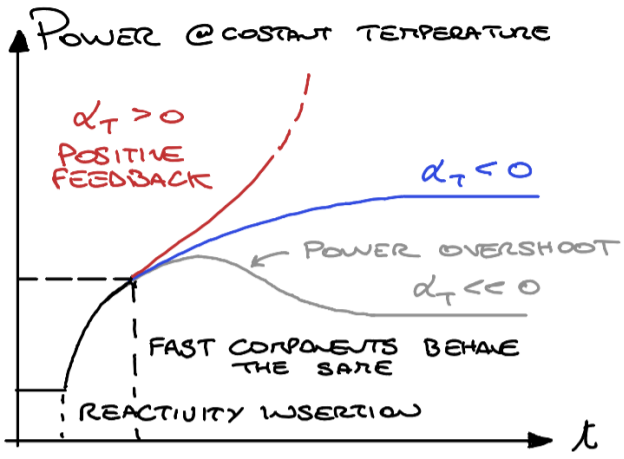

Figure 2.2: Overview of the effects of α on reactor power.

2.8 TRIGA Fuel

TRIGA fuel consists of Uranium-Zirconium Hydride (U-Zr-H), the solid moderator comprises hydrogen, with zirconium acting as the stabilizing element.

2.8.1 Experimental Findings

First Experiment: Mono-Energy Neutron Source

: Determination of the effective energy for moderation.

Second Experiment: Acoustical Resonance Study

: Influence of temperature on resonance peaks.

Third Experiment: Cross-Section Evaluation

: Measuring total removal cross-section.

2.9 Explanation of the Results

The findings from these experiments suggest that:

1. Hydrogen in a lattice has no free recoil.
2. The interference effect is characterized by a wavelength related to specific energy levels.
3. Possibility of up-scattering due to vibration modes.

2.10 Thermalization through Bounded Nuclei

The thermalization process occurs via two primary pathways:

1. **Translation Modes**:
   - Elastic interaction involving the entire crystal structure.
   - Reduced logarithmic energy decrease with increased temperature.
2. **Vibration Modes**:
   - Excitation of vibration states that influence up-scattering.
3. **Coherent and Incoherent Scattering**

The total scattering cross-section, $\sigma_{\text{scattering}}$, consists of both coherent and incoherent components:

$$\sigma_{\text{scattering}} = \sigma_{\text{coherent}} + \sigma_{\text{incoherent}} \tag{2.5}$$

In the TRIGA reactor

2.11 Elastic vs Inelastic Scattering

Elastic scattering involves no change in the internal quantum states of the scatterer. In contrast, inelastic scattering involves changes in these states.

- **Elastic**: No excitation states, such as with free hydrogen.
- **Inelastic**: Involves excitation related to vibrations and rotations within the molecule.

2.12 Thermalization through Bounded Nuclei

Thermalization of neutrons through bounded nuclei can occur via two primary mechanisms:

1. **Translation Modes**:
   - Elastic interactions that involve the entire crystal lattice.
   - Changes in temperature lead to variations in logarithmic energy decrease.
2. **Vibration Modes**:
   - Specific energy excitations related to vibrational modes.
   - Absorption of vibrational energy quanta can lead to up-scattering.

2.13 Coherent and Incoherent Scattering

Coherent scattering occurs when scattering events result in interference effects due to the crystal structure, manifesting as Bragg peaks. Incoherent scattering, in contrast, lacks such regular interference patterns.

$$\sigma_{\text{scattering}} = \sigma_{\text{coherent}} + \sigma_{\text{incoherent}} \tag{2.6}$$

2.14 Summary of Findings on TRIGA Fuel

The experimental findings on TRIGA fuel reveal key insights into moderation and reactivity:

- TRIGA fuel demonstrates effective moderation properties above a certain energy threshold.

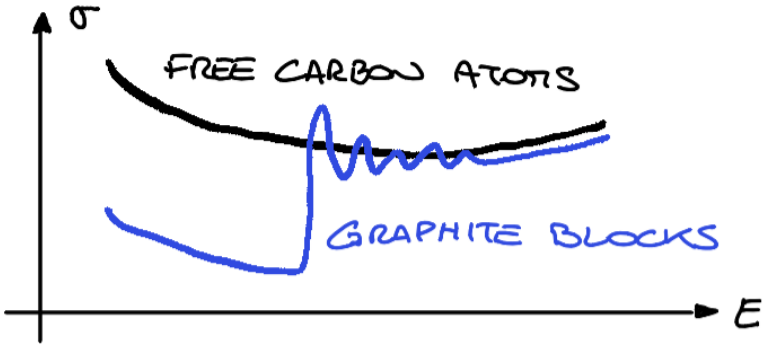

Figure 2.3: Coherent and incoherent scattering on Carbon atoms, when they form a crystalline structure in the graphite the scattering is inchoerent.

- The presence of zirconium hydride contributes significantly to the observed moderation effects.
- Doppler effects and up-scattering play important roles in spectral hardening.

2.15 Recap of Results

To summarize, the moderation capabilities of hydrogen in zirconium hydride are influenced by several factors, including lattice structure and vibrational modes. Based on experiments and Monte Carlo simulations:

- The Bragg peak is negligible in the energy range of interest.
- The primary mechanism involves vibrational modes related to the hydrogen lattice.
- Spectral hardening is observed with increasing temperature.

The findings suggest that Zr-H-based fuels exhibit complex moderation behavior, particularly at higher temperatures where vibrational modes play a significant role.

2.16 Additional Notes

2.16.1 Composition of fuel reactiviy coefficent in the TRIGA reactor

A breakdown of the contributions to α_f in the TRIGA reactor is presented in the table below.

Contribution	Aluminum Cladding	Stainless Steel Cladding
Doppler Effect	2.6	2.1
Spectral Hardening	5.7	7.8
Cell Flux Effect	3.5	5.7
Leakage Effect	2.2	2.1
Total α_f (pcm/°C)	8.3	9.9

Table 2.1: Breakdown of α_f contributions in TRIGA for different cladding materials.

2.16.2 TRIGA Fuel Characteristics

TRIGA fuel (Zr-H) can moderate up to 0.13 eV and can induce upscattering, as indicated by experimental evidence, which justifies the use of H_2O as a moderator.

- Hydrogen is bounded to Zr, and for thermal energy, the bound cannot be neglected.
- Hydrogen in Zr-H moderates mainly through inelastic scattering.
- **Model:** Using the Einstein quantum harmonic oscillator, we can explain the experimental evidence.

In TRIGA fuel, the temperature coefficient α_T is approximately -7 to -9 pcm/°C.

2.17 Experimental Brief

- **Step 1:** Shift out control rods $\rightarrow \rho \uparrow \rightarrow$ Power $\uparrow$
- **Step 2:** Overshoot of power is observed.
- **Step 3:** Compute the energy release up to the peak.
- **Step 4:** Estimate the temperature T.
- **Step 5:** Compute the temperature coefficient α_T.

Note: The coolant temperature coefficient, $\alpha_{T_{\text{coolant}}}$, is slightly positive.

2.18 Void Coefficient

2.18.1 Definition and Function

The void coefficient, α_v, is defined as:

$$\alpha_v = \frac{\partial \rho}{\partial \mathcal{E}} \tag{2.7}$$

where $\mathcal{E}$ represents the void fraction. The void coefficient plays an important role in safety, helping assess the response in situations like boiling, experiments, irradiation, and Loss of Coolant Accidents (LOCA).

2.18.2 Design Considerations and Physical Background

- Changes in moderation due to void formation lead to spectral hardening, causing a decrease in the resonance escape probability p.
- Absorption decreases, increasing the thermal utilization factor f.
- Leakage increases, reducing the probability of non-leakage P_{NL}.

Figure 2.4: Effect of moderation ratio on k_{eff}.

2.19 Impact on the Six-Factor Formula

- p: Resonance escape probability

$$\alpha_{p,i} = \ln\left(\frac{1}{p}\right)\left(\frac{1}{N_H V_H}\frac{\partial N_H V_H}{\partial V}\right) = \frac{\partial p}{\partial V} \tag{2.8}$$

- f: Thermal utilization factor

$$\alpha_{f,i} = (1-f)\left(-\frac{1}{N_H V_H}\frac{\partial N_H V_H}{\partial V}\right) \tag{2.9}$$

These coefficients are strongly dependent on absorption and moderation capacity. For example:

- **Void in Fuel** $\rightarrow \rho \downarrow$
- **Void in Water** $\rightarrow \rho \uparrow$

2.20 Experiment Outline

1. Start at zero power, aiming to create a void.
2. Ensure zero power, clean, and critical conditions.
3. Register control rod positions.
4. Insert a sample filled with water:
   - If $\alpha_v < 0$, $\rho \uparrow$
5. Return to criticality by adjusting the control rods.
6. Find control rod calibration curves to determine $\Delta\rho$.

Samples: Placed in one of the channels.

2.20.1 Examples of Void Experiments

- **In Ljubljana:** Bubbles were injected into the core. Monte Carlo simulations confirmed that $\alpha_v < 0$.
- **In Vienna:** Fuel elements with 70% enrichment were used, making $\alpha_v > 0$ due to high enrichment and the limited need for moderation.

2.21 Effects on Neutronics

The reactivity k can be expressed as:

$$k = \eta f \epsilon P_{NL} P_{NL} \tag{2.10}$$

The differential of k with respect to a parameter x_i can be expanded:

$$\alpha_i = \frac{\partial \rho}{\partial x_i} = \frac{1}{k}\frac{\partial k}{\partial x_i} = \frac{1}{\eta}\frac{\partial \eta}{\partial x_i} + \frac{1}{f}\frac{\partial f}{\partial x_i} + \frac{1}{\epsilon}\frac{\partial \epsilon}{\partial x_i} + \dots \tag{2.11}$$

- **Doppler Effect:** Variations in resonance weight due to self-shielding.
- **Spatial Self-Shielding:** Outer rings of the fuel pin shield the center, reducing the flux at the core.

2.22 Spectral Hardening

Spectral hardening occurs due to the harmonic oscillator behavior of Zr-H:

$$\alpha_{f,i} \approx \frac{1}{\Sigma_a^f}\frac{\partial \Sigma_a^f}{\partial x_i} - \frac{1}{\Sigma_a^m}\frac{\partial \Sigma_a^m}{\partial x_i} - \frac{1}{\phi}\frac{\partial \phi}{\partial x_i} \tag{2.12}$$

In fuel, spectral hardening increases the mean free path, affecting capture and escape probabilities.

2.22.1 Disadvantage Factor

$$\zeta = \frac{\phi_{\text{moderator}}}{\phi_{\text{fuel}}} \tag{2.13}$$

Since spectral hardening is stronger in the fuel, the ratio of escaping flux from the fuel is higher.

2.23 Experimental Procedure

This procedure yields a reactivity temperature coefficient rather than a prompt fuel coefficient.

- Measure ΔT due to $\Delta\rho$ and compute the ratio.
- No direct way to measure T_f (limited thermocouples, coolant contribution).

2.23.1 Simple Approach

1. Set reactor at desired power.
2. Record control rod position and extract positive reactivity.
3. Record power variation.
4. Calculate energy released until peak.
5. Calculate average temperature difference.

$$\Delta T_f = \frac{E}{G_f(N_f)} \tag{2.14}$$

6. Calculate the β temperature coefficient.

2.24 Coolant Effects

2.24.1 Components

Two contributions:

- Water density decrease, leading to $\rho \downarrow$
- Different rod capacity of H in water, leading to $\rho \uparrow$

Overall, $\alpha_{T_{\text{coolant}}} < 0$, although some contributions can be positive.

2.24.2 Isothermal Coefficient

$$\alpha_{\text{iso}} = \alpha_{T_f} + \alpha_{T_c} \tag{2.15}$$

Observed in Ljubljana by changing pool conditions while maintaining core conditions.

$$\alpha_{\text{iso}} = -3 + 6.5 = +3.5 \text{ pcm/°C} \tag{2.16}$$

Experimental Note: Despite positive contributions, $\alpha_{T_c} < 0$ overall.

3 Pulse Mode

3.1 Pulse Mode Operation

In pulse mode operation, the reactor is driven into a short, high-intensity power pulse. This mode is characterized by:

- Short duration
- High intensity

The observed parameters in pulse mode include:

1. Power (Intensity)
2. Time to reach peak power (to compare pulse duration)
3. Full Width at Half Maximum (FWHM) of the pulse

Figure 3.1: Graph illustrating pulse mode operation with parameters like peak power and FWHM.

3.2 Functions of Pulse Mode

Pulse mode can be used for various purposes, including:

- Activation analysis, including detector or semiconductor analysis
- Safety tests, such as reactivity insertion accidents
- Estimation of parameters related to reactor kinetics

3.3 Physical Background

In the pulse mode, the following sequence occurs:

$$\rho \uparrow\rightarrow P \uparrow\rightarrow E(T) \rightarrow T \uparrow\rightarrow \alpha_T \rightarrow \rho \downarrow\rightarrow \text{Feedback stabilizes the system.}$$

To translate energy into temperature, we need to know the heat capacity, C_p. The other important parameter is the temperature reactivity coefficient, α_f.

3.4 Experimental Evidence of Ljubljana Pulses

Videos of different reactivity insertions in the Ljubljana TRIGA reactor show that:

- Higher intensity in Cherenkov radiation correlates with larger $\Delta\rho$.
- Shorter pulses are achieved with larger $\Delta\rho$.
- The reactor is always scrammed after each pulse for safety, even if it's self-limited.

3.5 Nordheim–Fuchs Model

The Nordheim-Fuchs model is used to understand self-limited excursions over a short timespan. It relies on several assumptions:

1. Transient modeled with point kinetics
2. Delayed neutrons are neglected
3. $\Delta\rho$ is considered a step function
4. Adiabatic model for energy balance

(3.1)

Figure 3.2: Power pulse prediction by Nordheim-Fuchs model showing peak power and pulse duration.

3.6 Power Pulse Parameters

The key parameters of a power pulse are:

- $\Delta\rho$: Known insertion value
- T_f: Fuel temperature from instrumentation
- E_{released}: Power integral for total energy release

3.7 Why TRIGA Can Operate in Pulse Mode

The TRIGA reactor can safely operate in pulse mode due to:

- Large prompt and negative temperature coefficient, $\alpha_f = -8$ to -10 pcm/K
- High heat capacity of the fuel-moderator combination

> **Note:** In the Ljubljana TRIGA reactor, fewer control rods and elements with higher uranium content allow a unique pulse operation configuration.

3.8 Physical Phenomenon of the Pulse

The physical phenomenon during a pulse involves:

Figure 3.3: Graph showing power pulse parameters and energy release.

1. Large ρ insertion (> 2)
2. Prompt supercriticality reached
3. Fuel temperature increases, causing $\rho \downarrow$ until stability

3.9 Power Pulse Parameters

The parameters for a power pulse are typically:

- ΔP: Known insertion level
- T_f: Measured from instrumentation
- E_{released}: Calculated from power integral

3.10 Examples and Limitations

Examples of the results from the Nordheim-Fuchs model indicate:

- Increasing ρ_0 leads to higher peak power, reduced FWHM, increased energy in fuel, and larger ΔT_f.

Limitations of this model include:

- Valid only for short pulses (delay of neutrons is negligible)

Figure 3.4: Illustration of power and energy evolution in pulse mode.

- Incomplete modeling of the temperature dependency

Note: The Nordheim-Fuchs model requires validation and verification against experimental data for accurate results.